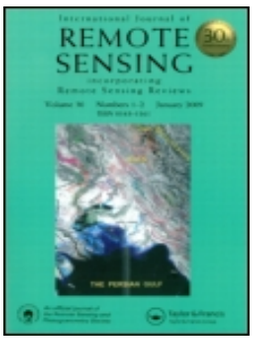

International Journal of Remote Sensing

ISSN: 0143-1161 (Print) 1366-5901 (Online) Journal homepage: https://www.tandfonline.com/loi/tres20

Height and biomass of mangroves in Africa from ICESat/GLAS and SRTM

Temilola E. Fatoyinbo & Marc Simard

To cite this article: Temilola E. Fatoyinbo & Marc Simard (2013) Height and biomass of mangroves in Africa from ICESat/GLAS and SRTM, International Journal of Remote Sensing, 34:2, 668-681, DOI: 10.1080/01431161.2012.712224

To link to this article: https://doi.org/10.1080/01431161.2012.712224

International Journal of Remote Sensing
Vol. 34, No. 2, 20 January 2013, 668–681

Taylor & Francis
Taylor & Francis Group

Height and biomass of mangroves in Africa from ICESat/GLAS and SRTM

Temilola E. Fatoyinbo[a]* and Marc Simard[b]

[a]*Biospheric Sciences Laboratory, NASA Goddard Space Flight Center, Greenbelt, MD 20771, USA;* [b]*Radar Systems, Jet Propulsion Laboratory, California Institute of Technology, Pasadena, CA, USA*

(*Received 1 November 2010; accepted 1 January 2012*)

The accurate quantification of the three-dimensional (3-D) structure of mangrove forests is of great importance, particularly in Africa where deforestation rates are high and the lack of background data is a major problem. The objectives of this study are to estimate (1) the total area, (2) canopy height distributions, and (3) above-ground biomass (AGB) of mangrove forests in Africa. To derive the 3-D structure and biomass maps of mangroves, we used a combination of mangrove maps derived from Landsat Enhanced Thematic Mapper Plus (ETM+), lidar canopy height estimates from ICESat/GLAS (Ice, Cloud, and land Elevation Satellite/Geoscience Laser Altimeter System), and elevation data from SRTM (Shuttle Radar Topography Mission) for the African continent. The lidar measurements from the large footprint GLAS sensor were used to derive local estimates of canopy height and calibrate the interferometric synthetic aperture radar (InSAR) data from SRTM. We then applied allometric equations relating canopy height to biomass in order to estimate AGB from the canopy height product. The total mangrove area of Africa was estimated to be 25,960 km^2 with 83% accuracy. The largest mangrove areas and the greatest total biomass were found in Nigeria covering 8573 km^2 with 132×10^6 Mg AGB. Canopy height across Africa was estimated with an overall root mean square error of 3.55 m. This error includes the impact of using sensors with different resolutions and geolocation error. This study provides the first systematic estimates of mangrove area, height, and biomass in Africa.

1. Introduction

The measurement of forest biomass is crucial for carbon cycle and climate change studies. However, the amount and distribution of forest biomass is still poorly understood. Global estimates of terrestrial biomass range from 385×10^9 to 650×10^9 Mg and forests alone hold about 70–90% of the terrestrial biomass (Houghton, Hall, and Goetz 2009). Mangrove forests cover only about 1% of the Earth's terrestrial surface, but they are amongst the highest carbon-storing and carbon-exporting ecosystems globally (Dittmar et al. 2006; Donato et al. 2011).

Estimating the distribution and biomass of mangrove forests is challenging due to the complex physical environment of these forests. They are constantly inundated by diurnal tides and the characteristic above-ground roots often hinder *in situ* measurements.

*Corresponding author. Email: lola.fatoyinbo@nasa.gov

ISSN 0143-1161 print/ISSN 1366-5901 online

http://dx.doi.org/10.1080/01431161.2012.712224
http://www.tandfonline.com

Large-scale field measurements of mangroves are therefore rare to non-existent. The measurements that do exist are usually tailored towards a particular study, and the sampling and measurement methodologies vary. In Africa, studies of mangroves have focused on forest composition and zonation (Ukpong 1995; De Boer 2002; Adams, Colloty, and Bate 2004; Dahdouh-Guebas et al. 2004b), management and utilization of mangrove products (Traynor and Hill 2008; Crona et al. 2009), the degradation of mangroves (Kruitwagen et al. 2008), and the ecology of mangrove-associated fauna (Faunce and Serafy 2006). Recent assessments of mangrove cover in Africa are mostly limited to small areas, which makes the comparison with countrywide statistics difficult (Dahdouh-Guebas et al. 2004b). With the emergence of new remote-sensing methodologies, it is now possible to map the spatial distribution and three-dimensional (3-D) structure of mangroves systematically (Simard et al. 2006, 2008; Lucas et al. 2007; Fatoyinbo et al. 2008).

Optical remote-sensing techniques have been proved to be a reliable tool for the estimation of mangrove forest areas globally, as shown by the large number of studies (Aschbacher et al. 1995; Smith et al. 1998; Dahdouh-Guebas et al. 2000; Kovacs, Wang, and Blanco-Correa 2001; Dahdouh-Guebas et al. 2002; Sulong et al. 2002; Cohen and Lara 2003; Wang et al. 2003; Gesche et al. 2004; Satyanarayana et al. 2001). The most comprehensive database of global mangrove cover is maintained by the UNEP World Conservation Monitoring Centre, which published the World Mangrove Atlas (Spalding, Blasco, and Field 1997). This database is based on a review of the mangrove literature and mangrove cover estimated from multiple studies, data sets, and methodologies.

For Africa in particular, the data, methodologies, and time frame used to generate the mangrove maps vary greatly, and a systematic methodology is needed to derive mangrove cover estimates. An updated version of global maps has recently been published (Giri et al. 2011). However, to obtain a 3-D structure and biomass, in addition to spatial distribution, active remote sensing from lidar and interferometric synthetic aperture radar (InSAR) is the best measurement tool available.

The only global InSAR and lidar data sets currently available are from the spaceborne SRTM (Shuttle Radar Topography Mission) and ICESat/GLAS (Ice, Cloud, and land Elevation Satellite/Geoscience Laser Altimeter System). The SRTM (Farr et al. 2007) was flown aboard the Space Shuttle Endeavour in February 2000 (Rodriguez, Morris, and Belz 2006). The SRTM measured terrain topography using dual-antennae C-band InSAR, covering areas from 56° S and 60° N. SRTM data are freely available at 1 arcsecond (30 m) resolution for the USA and at 3 arcsecond (90 m) resolution globally. The SRTM DEM (digital elevation model) is the most accurate, globally consistent elevation data set covering 80% of the Earth's landmasses. The SRTM height measurement is in fact biased by vegetation structure and can therefore be used to estimate canopy height (Kellndorfer et al. 2004). The GLAS instrument recorded full-waveform altimetry data using a 1064 nm laser that operated from 2003 to 2009. The lidar footprints have an approximate diameter of 70 m, and are separated by 172 m along track (Schutz et al. 2005). In tropical regions, sampling is greatly hindered by consistent cloud cover. Although it was primarily a mission designed for the measurement of ice-sheet dynamics, it has been used to measure vegetation structure (Lefsky et al. 2005, 2007; Rosette et al. 2010). Previous work in the Santa Marta region of Colombia (Simard et al. 2008) has shown the possibility of using spaceborne InSAR and lidar data integration to measure the 3-D vegetation structure and biomass of mangroves.

The objectives of this study are to (1) estimate mangrove heights on a continental scale from InSAR and lidar integration, (2) estimate the total AGB of mangrove forests in Africa, and (3) estimate the associated errors in our measurements. In this study, we

produce the first continental-scale maps of the spatial distribution, 3-D structure, and AGB of mangroves in Africa. We address new challenges introduced by large-scale mapping that are related to the variety of the biogeographical setting as well as the accuracy and sampling of data.

2. Materials and methods

2.1. Study areas

In continental Africa, mangroves grow in coastal areas ranging from Mauritania (19° N) in the northwest to Angola (10° S) in the southwest, and from South Africa (29° S) in the southeast to Egypt (28° N) in the northeast, including Madagascar. On the Atlantic coast of Western Africa, there are a total of seven indigenous species plus one introduced mangrove palm, *Nypa fruticans*, which are also found on the Atlantic and Pacific coasts of the Americas (Spalding, Blasco, and Field 1997). The indigenous species are *Acrostichum aureum*, *Avicennia germinans*, *Conocarpus erectus*, *Laguncularia racemosa*, *Rhizophora harrisonii*, *R. mangle*, and *R. racemosa.* The distribution limit of mangroves coincides with arid regions with rainfall below 30 mm year^{-1} (Saenger and Bellan 1995).

On the Indian Ocean and Red Sea coastlines, the mangrove area is relatively small compared to the total length of the coastline, due to very arid conditions in areas north of the equator. There are 14 species of mangrove present in this area, which differ from the west coast species. They are *Acrostichum aureum*, *Avicenna marina*, *Bruguiera cylindrical*, *B. gymnorrhiza*, *Ceriops tagal*, *Excoecaria agallocha*, *Heritiera littoralis*, *Lumnitzera racemosa*, *Pemphis acidula*, *R. mucronata*, *R. racemosa*, *Sonneratia alba*, *S. caseolaris*, and *Xylocarpus granatum*. The largest diversity on the continent is found in Mozambique, where 10 of the species are present (Spalding, Blasco, and Field 1997).

2.2. Mangrove extent from Landsat

Landsat TM GeoCover data were acquired from the University of Maryland Global Land Cover Facility (http://glcf.umd.edu). The GeoCover data set consists of Landsat data that have near global coverage and are available for three time periods ranging from 1973 to 2001. The Landsat ETM data used in this study had been orthorectified and georeferenced (Tucker, Grant, and Dykstra 2004).

A total of 117 Landsat Enhanced Thematic Mapper Plus (ETM+) scenes from 1999 to 2002 were subset to include only low-elevation coastal areas where mangroves may be present. All areas with elevations lower than 40 m were identified using the SRTM DEM. An unsupervised Iterative Self-organizing Data Analysis (ISODATA) classification was then applied to each Landsat image subset to discriminate mangroves from other types of vegetation (Green et al. 1998; Fatoyinbo et al. 2008). The classification was filtered using previously published maps, the World Mangrove Atlas (Spalding, Blasco, and Field 1997), visual inspection, and high-resolution imagery from Google Earth software. The resulting classes were manually combined into a final classification with four land-cover types (mangrove, other vegetation, bare ground, and water). In mangrove forests in Central Africa, in particular Gabon and the Democratic Republic of Congo, no cloudless Landsat scenes were available. In these areas with persistent cloud cover, we had to use cloud-free Landsat data from 1989.

There are no local maps with known accuracy or sufficient field data available to assess relative accuracy. Therefore, we based our estimation of classification accuracy on an independent and systematic method for selecting validation points. We used points separated

by 900 m (10 pixels) along a north–south running transect. The points were also spaced by 0.5° longitude for the coast running from Senegal to Nigeria. For the remaining areas, we used points separated by 900 m along an east–west running transect and spaced by 0.5° latitude. We assessed mapping accuracy by visual interpretation of high-resolution images in Google Earth software. We used only those points that were classified or identified as mangroves on the land-cover map or in Google Earth.

2.3. Measurement of tree height from lidar–InSAR fusion

ICESat/GLAS waveforms were acquired from the National Snow and Ice Data Center (NSIDC) website (http://nsidc.org/data/icesat). We used the GLA14 (Global Land surface Altimetry) data product to estimate canopy height. A total of 327 waveforms were used to estimate tree height in this study, as GLAS footprints were not available in all mangrove areas. GLAS data were available for sites in Senegal, Gambia, Guinea Bissau, Guinea, Nigeria, Cameroon, Gabon, Congo, Angola, Mozambique, Tanzania, Kenya, Eritrea, and Madagascar.

The GLA14 product was produced by fitting up to six Gaussian distributions to the GLAS lidar waveform (Zwally et al. 2003). The shape and position of the Gaussian distributions describe the vertical structure of the canopy within the lidar footprint. It is generally assumed that the Gaussian peak furthest from the sensor is the ground return and the beginning of the waveform signal (i.e. first return with voltage above the noise level) is the return from the top of the canopy (Harding and Carabajal 2005). The cumulative distribution (i.e. percentile) of the energy within the waveform is generally used to describe the vertical distribution of scatterers (e.g. leaves and branches) within the canopy. The percentile is computed from the beginning of the waveform (i.e. last return with voltage above the noise level). Relative height (rh_x) is defined as the distance between the point where the percentile energy reaches x (where x is the percentile value) and the location of the ground peak defined as rh_0 (Lefsky et al. 2005, 2007). Figure 1 shows an example of a waveform and the location of GLAS footprints used.

We used only data from cloud-free profiles and excluded all waveforms that did not have suitable data for determining tree heights. We excluded waveforms with a single Gaussian peak, which generally meant that the footprint was over water or bare soil areas. We also excluded waveforms with low signal-to-noise ratios (i.e. below 50), which may have been reflected from clouds, or where Gaussian fits may include noise peaks. We found high signal-to-noise ratios up to 300 in the GLAS data.

SRTM version 4 data were downloaded from the Consultative Group for Agricultural Research (CGIAR). We used 30 SRTM scenes to build a single SRTM DEM covering the coast of Africa mosaic. Using the mangrove land-cover map, we masked all non-mangrove areas on the SRTM DEM. This resulted in an uncalibrated height map of the mangrove areas. In forests, the C-band radar signal penetrates into the canopy to scatter with all forest components and the ground. Thus, the radar height estimate (i.e. radar phase centre) lies somewhere within the canopy volume, which can be used to estimate canopy height (Kellndorfer et al. 2004; Gillespie et al. 2006). Based on the reasonable assumption that mangroves are located at sea level, the elevation measured by SRTM (i.e. phase centre) is directly related to canopy height and can be calibrated to estimate the canopy height of mangrove forests (Simard et al. 2006).

The SRTM pixels corresponding to the GLAS shots were extracted (Figure 1). We assumed that rh_{75} represents the canopy height and derived linear regressions between the GLAS point's rh_{75} values (relative height of the canopy at the 75th percentile minus rh_0) and the DEM height (H_{SRTM}) values to determine the regression equation of the form

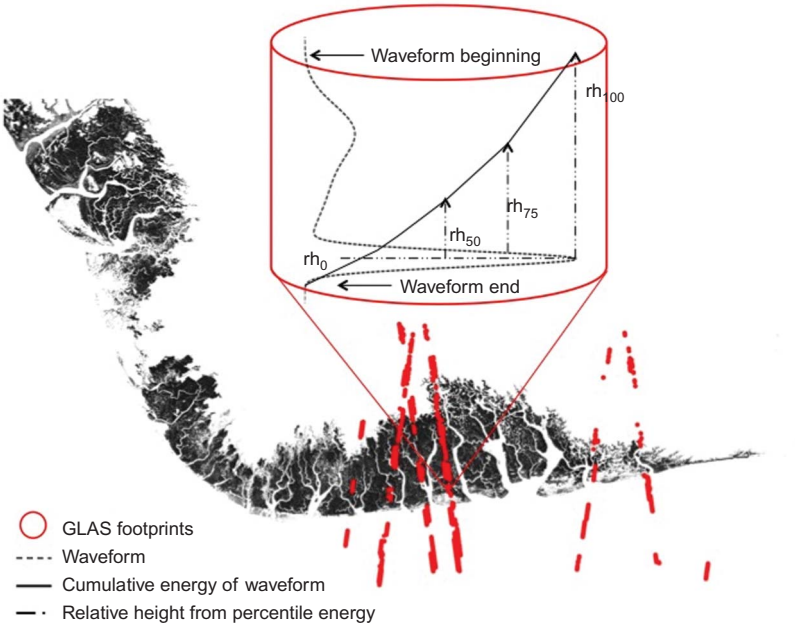

Figure 1. GLAS footprint coverage over the Niger Delta mangrove ecosystem.

Note: Within each footprint, a waveform representing the canopy and ground profile is extracted to derive tree canopy height.

$$\mathrm{rh}_{75} = a \times H_{\mathrm{SRTM}} + b, \tag{1}$$

where a is the slope of the regression and b is the y intercept in metres. Studies of forest biomass worldwide have shown that there is a strong correlation between tree size, in terms of diameter and height, and tree biomass. In general, the diameter at breast height (DBH) of a tree is the strongest predictor of AGB (Chave et al. 2005). For mangrove forests, a global stand height–biomass allometric equation was calculated by Saenger and Snedaker (1993):

$$\text{biomass } \left(\mathrm{Mgha}^{-1}\right) = 10.8 \times H(\mathrm{m}) + 35. \tag{2}$$

This equation was obtained from 43 field data sets distributed globally $R^2 = 0.59$ and root mean square error (RMSE) = 43.8). To compute total AGB and AGB distribution of mangroves on the continental scale, we used rh_{75} and Equation (2) to derive the biomass values as this equation was computed for a large range of tree heights and was derived to be applicable globally.

3. Results and discussion

All of the results were calculated and mapped on a per country basis to facilitate comparison with previously published results and data distribution. The maps are freely available for Google Earth software at http://www-radar.jpl.nasa.gov/coastal.

3.1. Mangrove land-cover map

The total area of mangrove cover in Africa was found to be 25,960 km^2 with 83% accuracy. The five largest mangrove areas – in decreasing order – were found in (1) Nigeria, (2) Mozambique, (3) Guinea Bissau, (4) Madagascar, and (5) Guinea. The smallest area of mangroves is found in Mauritania at 0.4 km^2. Nigeria, with a mangrove area of 8573 km^2, has the fourth largest mangrove area in the world, after Indonesia, Brazil, and Australia. The overall accuracy of the land-cover map was 83%, considering 10% omissions and 7% commissions, based on a total of 540 points (Table 1). The main sources of error in the land-cover map were due to difficulties in distinguishing between mangrove forests and other forest types, such as coastal forests or rainforests, and the presence of clouds, especially in the equatorial regions. In Central Africa, the map accuracy was much lower, at 68%, due to the high cloud cover. The land-cover maps for Nigeria, Cameroon, Tanzania, and Kenya are presented in Figure 2 and the breakdown of mangrove area by state is presented in Table 2.

Although it is not our objective to assess changes in the spatial extent of mangroves over time, it is important to compare our results with previous studies. Overall, the land-cover maps show that the mangrove area of Africa is smaller than the previously estimated

Table 1. Confusion matrix of mangrove land-cover classification in Africa.

	Truth land cover		
Class	Mangrove	Non-mangrove	Total
Mangrove	449	39	488
Non-mangrove	52	0	52
Total	501	39	540

Note: The overall accuracy was 83% with 10% omissions and 7% commissions.

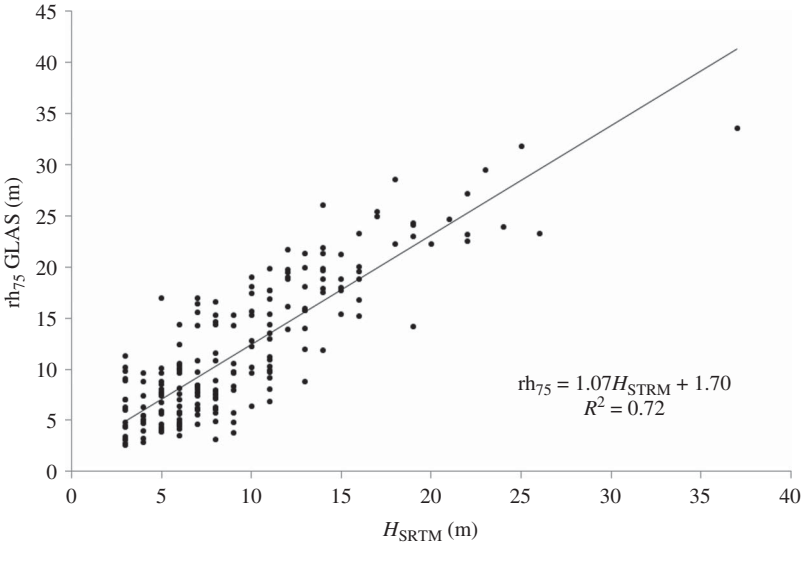

Figure 2. Canopy height regression between GLAS rh_{75} and SRTM phase centre to calibrate the SRTM DEM.

Table 2. Area of mangrove cover and mean biomass per hectare per country.

Country	Area (km^2)	Total biomass (Mg)	Mean biomass (Mg ha^{-1})
Angola	154	1,441,200	93
Benin	18	137,719	76
Cameroon	1,483	25,334,900	171
Congo	15	267,603	178
Côte d'Ivoire	32	406,516	124
Djibouti	17	1,653,170	90
DRC	183	51,570	140
Egypt	1	8344	117
Equatorial Guinea	181	2,922,420	161
Eritrea	49	640,038	129
Gabon	1,457	23,840,000	162
Gambia	519.11	5,509,300	106
Ghana	76	742,925	97
Guinea	1,889	18,153,800	108
Guinea Bissau	2,806	31,712,300	113
Kenya	192	2,294,820	119
Liberia	189	2,141,860	113
Madagascar	2,059	24,856,900	121
Mauritania	0.4	4156	95
Mozambique	3,054	30,974,100	101
Nigeria	8,573	94,788,000	111
Senegal	1,200	11,462,100	95
Sierra Leone	955	10,655,600	112
Somalia	30	436,907	143
Sudan	4	135,626	113
South Africa	12	40,018	100
Togo	2	15,861	78
Tanzania	809	11,037,800	136
Africa	25,960	301,665,553	116

30,000 km^2 (Spalding, Blasco, and Field 1997; FAO 2007). However, the exact estimate of changes in mangrove area due to natural and anthropogenic disturbances cannot be calculated because of the differences in data collection methodologies, the variations in the definition of mangrove forests, and the differences in the resolution of the data sets used in the previous estimates. The large decreases in mangrove area estimates are in part due to degradation in mangrove area but also due to different definitions of 'mangrove areas'.

In many studies, mangrove area was overestimated because it was difficult to differentiate between mangrove forests and adjacent mudflats, salt marshes, swamp forests, and bare areas using low-resolution data (1 km × 1 km). In many tropical areas there is consistent cloud cover that results in poor coverage from optical data. This is the case in many of the tropical regions, with extreme discrepancies in Congo and Côte d'Ivoire for example. Furthermore, certain studies include the 'mangrove palm' *N. fruticans* as a mangrove species, whereas other studies do not. In this study, we did not include bare ground and mudflats and also did not count uniform *Nypa* stands as mangrove areas as much as possible. Other very large differences in area measurement such as in Egypt, Côte d'Ivoire, and Sudan are probably due to a lack of up-to-date studies and remotely sensed data leading to poor mapping capabilities at the time of the study.

A direct comparison or estimation of the amount and rate of decrease or degradation in mangrove area throughout Africa is difficult, but we know that mangrove areas

have decreased on the continent due to anthropogenic influences. Over 60% of Nigeria's mangrove stands are found in the Niger Delta region, yet studies in the Niger Delta have shown that mangroves have greatly suffered from the development and rapid increase in oil and gas exploitation in the area and the resulting pollution by oil spills, rapid urbanization, and dredging of canals, as well as the introduction of the invasive mangrove palm *N. fruticans* (James et al. 2007). In general, decreases in mangrove area in West Africa are primarily attributed to anthropogenic pressures in coastal regions leading to conversion of land use for the production of salt and rice, urban and tourism development, pollution, lack of sustainable resource management, and recently, the development of shrimp aquaculture (FAO 2007). In eastern Africa, large decreases in mangrove areas are primarily due to felling for household products and conversion to urban, agricultural, and touristic areas and diversion of fresh water from damming. These measurement inconsistencies justify the need for a systematic approach to mangrove mapping as presented in this study.

3.2. *Height and biomass measurements*

The GLAS–SRTM calibration regression is shown in Figure 2. The resulting linear fit between the height estimates from rh_{75} and the SRTM DEM is

$$rh_{75} = 1.07 \times H_{SRTM} + 1.70. \quad (3)$$

The RMSE is 3.55 m. Calibrated canopy height maps for West and East Africa are presented in Figure 3. In previous studies, a comparison of SRTM-derived canopy height with field and airborne lidar data yielded RMSEs of 1.6 and 2.0 m, respectively (Simard et al. 2006; Fatoyinbo et al. 2008). Our results are very similar to these studies. These are the lowest errors that can be achieved using data fusion of these lidar and radar sensors without the incorporation of field validation.

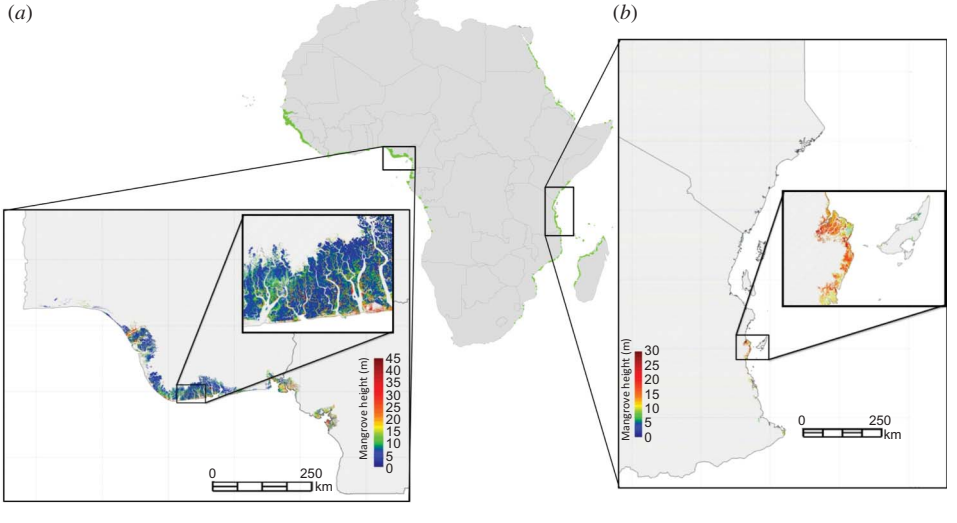

Figure 3. SRTM canopy height maps of Nigeria–Cameroon (*a*) and Kenya–Tanzania (*b*).
Note: The overall extent of mangrove forests is shown in green.

Based on our results, the equatorial areas of Africa are best suited for the growth of tall mangroves but not for their expansion, since the actual mangrove area is small in these countries. Average biomasses per country ranged from 76 Mg ha^{-1} in the Republic of Benin to 178 Mg ha^{-1} in Congo. The greatest total biomass values were found in Nigeria and Guinea Bissau and the lowest in Mauritania.

Previous studies of the canopy height, biomass, and distribution of mangroves have shown that geographical setting is more important in determining mangrove structure and distribution than the latitudinal distribution (Fatoyinbo et al. 2008). This is particularly evident on the African continent, and especially in West Africa, where a great proportion of mangroves grow within a small range of latitudes, but the forest area and structure vary greatly. In Nigeria, mangroves are extensive and canopy height can be very tall, but in adjacent Benin and Togo, their distribution is very limited and canopy height is short. In Senegal, Gambia, Guinea Bissau, and Guinea, mangroves extend very far inland, up to 160 km in Gambia, but at the same latitudes in East Africa, in Somalia, Djibouti, and Eritrea, mangrove forests are sparse. Estuaries and deltas with extensive freshwater supply are the most advantageous for mangrove growth, in terms of both height and extent, and have a much greater influence than latitude. Indeed, all of the mangrove forests with large areas, tall trees, and/or high biomass grow either in estuaries or in deltas.

3.3. Error analysis

The fact that we used three different data sets in this study also increases the incidence of error in our calculations. In the land-cover classification, we observed 83% accuracy, with 17% errors from commissions and omissions from the classification. The systematic error (i.e. bias) from the calibration equation was low at 1%.

Cloud cover was a major source of error, especially in central African nations, where cloud cover is persistent. Some systematic but localized errors in the SRTM DEM resulted in overestimation of tree height and biomass, but also in the omission of mangrove areas. For example, on an island in the Niger Delta, the DEM indicated that canopy height was 363 m. This is a common error with the SRTM DEM on islands, which may have been caused by difficulties in SRTM interferometric phase unwrapping (i.e. the method to retrieve elevation from the radar interferometric phase). Because this measurement was too high for mangroves, this area was omitted from the height and biomass estimation.

The geolocation error of the GLAS instrument ranges from 4.6 to 53.4 m (according to NSIDC), which greatly influences the accuracy of height measurement, particularly if the canopy is heterogeneous. The actual height derived from the GLAS waveform may therefore not correspond to the mean canopy height of the SRTM pixel that is measured. The height estimated from the lidar waveform is affected by forest composition and heterogeneity as canopy shape, reflective properties, and the associated photon interactions all influence the structure of the waveform (North et al. 2010; Rosette et al. 2010). In addition, the waveform is most sensitive to the footprint centre, since laser gain decreases with distance from the centre of the footprint. Mangrove forests are characterized by distinct ‘zones’ that are dependent on the location relative to the coast or river and that show great heterogeneity in forest structure, type, and composition (Tomlinson 1994). When the GLAS footprint is close to the border of two zones, this can result in large discrepancies in height measurement (Figure 4). Although low in species composition, mangrove forests are very heterogeneous, ranging from tall, dense forests to very short, sparse, shrubby areas within a few hundred metres. The 70 m GLAS footprint is not always able to characterize this

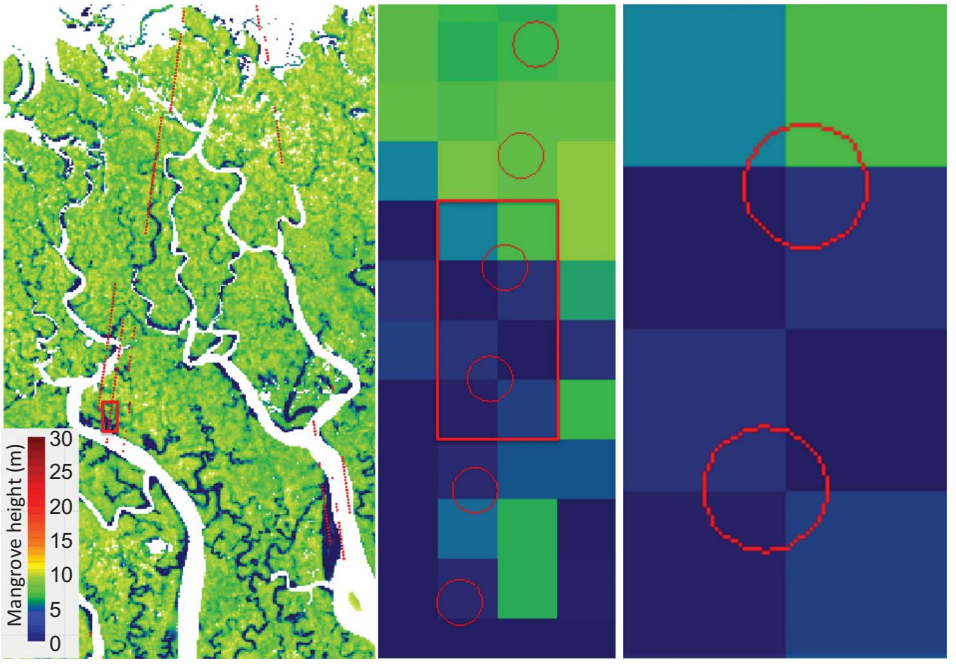

Figure 4. GLAS footprint locations (in red) on an SRTM height map.

Note: The two zoomed images on the right show that while the mean height value given by a footprint is that of the SRTM pixel where the centre of the shot is located, the actual area measured by GLAS can be in several SRTM pixels, resulting in height measurement error.

heterogeneity, resulting in discrepancies with SRTM measurements. For example, when looking at the variance within a seemingly homogeneous forest in Cameroon, we found that within a single 1 km^2 patch, the standard deviation of canopy height was 5 m, showing that the height within a forest can vary greatly within a small area (Figure 4). Therefore, since the trees measured by SRTM and GLAS are not exactly the same, the differences between height measurements and what we state as the error of measurement are inflated. The differences in physical parameters measured by radar and lidar, in addition to differences in resolution, also increase the height and biomass estimation error. These combinations of sources of error are illustrated in Figure 5.

The identification of the ground location within the waveform influences the estimate of canopy height and therefore also of biomass. In tidal forests, such as mangroves, the height of the ground or of the water level may vary depending on the tidal level. This may influence the GLAS ground return signal and therefore the relative height estimates. On the other hand, microtopographic features will most likely average out by selecting the furthest Gaussian peak as the ground. In this study, we chose to use rh_{75} as the height of the canopy, as this measurement resulted in the lowest error compared to the SRTM measurement.

The RMSE of Equation (3) is 65.4 Mg ha^{-1}. This error is high due to large variability in the measurements made and the natural variability of the data set. Since this is a global equation, it does not take into account local variability in height and biomass. There is generally a great amount of uncertainty when working with height–biomass allometric equations. Because height is not the most direct indicator of tree biomass (Chave et al. 2005), some error is always introduced into the estimate when deriving biomass from

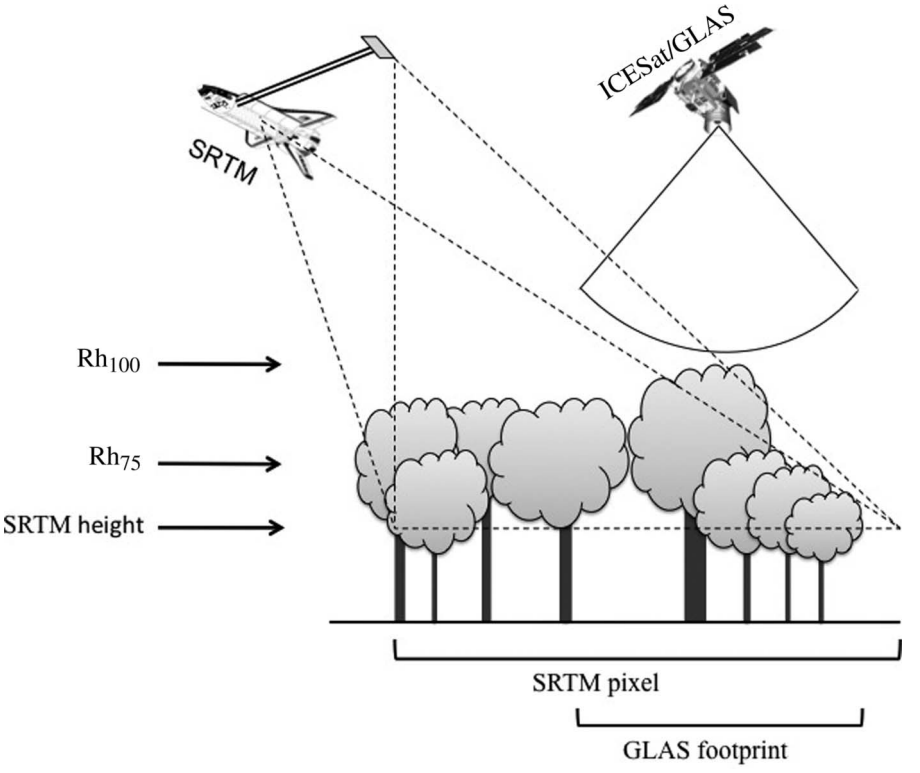

Figure 5. Example of differences in measurements by the two active radar and lidar sensors, which shows that the heterogeneity of forest structure within an SRTM pixel and a GLAS footprint can result in different height measurements from each sensor.

height. To obtain more accurate measurements of biomass from radar and lidar data, it is crucial that more reliable allometric equations are developed as a function of vertical structure parameters.

4. Conclusions

Mangroves are one of the most important ecosystems in coastal areas in terms of ecology and economy, but they are still being destroyed and degraded at great rates. The lack of field studies and homogeneous historical data has made the calculation of rates of change in mangrove cover difficult. In this article, we produced the first systematic estimate of mangrove cover, structure, and biomass for the entire African continent and Madagascar. This map can now be used as a baseline, as the techniques used in this article allow recalculation and reproduction with updated estimates of canopy height and allometry in Africa as well as comparison with the rest of the world.

The total area of mangrove forest in Africa for the period of 1999–2000 based on the classification of Landsat ETM+ images is 25,960 km^2, with the largest area found in Nigeria at 8573 km^2 and the smallest area in Mauritania with 0.4 km^2. The overall accuracy of the map was 83%, considering 10% omissions and 7% commissions. This overall estimate is lower than previous estimates of mangrove cover in the World Mangrove Atlas (Spalding, Blasco, and Field 1997), mostly due to classification errors from high cloud cover and difficulties in distinguishing between mangroves and adjacent forests. We do

believe that there is an overall decrease in mangrove cover that can be attributed to deforestation and degradation of mangroves from anthropogenic pressures; however, we cannot accurately quantify the rate and percentage decrease in area because of the differences in methodology and data sets used in the various published estimates.

Since mangrove ecosystems are relatively homogeneous and mangroves grow on flat terrain at sea level, the results from this study are some of the most accurate results we can expect from a radar/lidar integration study. The height maps derived from SRTM and GLAS data confirmed this type of data fusion to measure mangrove canopy height to be appropriate, with an average RMSE of 3.55 m. This value includes the impact of canopy heterogeneity on the remote-sensing measurement that is not geolocated. Previous studies using SRTM and lidar data sets in Colombia measured canopy height with an accuracy of 2.7 m (Simard et al. 2008). When similar methods using lidar were combined with field data, the RMSE decreased to 1.6 m in Mozambique (Fatoyinbo et al. 2008). To achieve even higher accuracy, or lower error, field validation of mangrove height and biomass calibration should therefore be included in future studies.

Overall, only 327 usable GLAS footprints were found for all mangrove areas in Africa. This is a very small sample size covering only 0.02% of the total mangrove area. This is, however, the greatest number of systematic height measurements available. GLAS was not optimized for vegetation measurement, but as the only spaceborne lidar, it is the only data set available for continental-scale studies. We look forward to the future lidar and InSAR missions, which will provide greater coverage over forested areas.

Acknowledgements

Dr Fatoyinbo would like to thank the National Aeronautics and Space Administration (NASA) Postdoctoral Program for funding this research. The work presented in this article was conducted at the Jet Propulsion Laboratory, California Institute of Technology, under contract with NASA, and at the NASA Goddard Space Flight Center.

References

Adams, J. B., B. M. Colloty, and G. C. Bate. 2004. "The Distribution and State of Mangroves along the Coast of Transkei, Eastern Cape Province, South Africa." *Wetlands Ecology and Management* 12: 531–41.

Aschbacher, J., R. Ofren, J.-P. Delsol, T. B. Suselo, S. Vibulsresth, and T. Charuppat. 1995. "An Integrated Comparative Approach to Mangrove Vegetation Mapping Using Advanced Remote Sensing and GIS Technologies: Preliminary Results." *Hydrobiologica* 295: 285–94.

Chave, J., C. Andalo, S. Brown, M. A. Cairns, J. Q. Chambers, D. Eamus, H. Fölster, F. Fromard, N. Higuchi, T. Kira, J.P. Lescure, B.W. Nelson, H. Ogawa, H. Puig, B. Riera, and T. Yamakura. 2005. "Tree Allometry and Improved Estimation of Carbon Stocks and Balance in Tropical Forests." *Oecologia* 145: 87–99.

Cohen, M. C. L., and R. N. J. Lara. 2003. "Temporal Changes of Mangrove Vegetation Boundaries in Amazonia: Application of GIS and Remote Sensing Techniques." *Wetlands Ecology and Management* 11, no. 4: 223–31.

Crona, B. I., P. Rönnbäck, N. Jiddawi, J. Ochiewo, S. Maghimbi, and S. Bandeira. 2009. "Murky Water: Analyzing Risk Perception and Stakeholder Vulnerability Related to Sewage Impacts in Mangroves of East Africa." *Global Environmental Change* 19: 227–39.

Dahdouh-Guebas, F., R. De Bondt, P. D. Abeysinghe, J. G. Kairo, S. Cannicci, L. Triest, and N. Koedam. 2004b. "Comparative Study of the Disjunct Zonation Pattern of the Grey Mangrove *Avicennia marina* (Forsk.) Vierh. in Gazi Bay Kenya." *Bulletin of Marine Science* 74: 237–52.

Dahdouh-Guebas, F., I. Van Pottelbergh, J. G. Kairo, S. Cannicci, and N. Koedam. 2004a. "Human-Impacted Mangroves in Gazi Kenya: Predicting Future Vegetation Based on Retrospective Remote Sensing, Social Surveys, and Tree Distribution." *Marine Ecology Progress Series* 272: 77–92.

Dahdouh-Guebas, F., A. Verheyden, W. De Genst, S. Hettiarachchi, and N. Koedam. 2000. "Four Decade Vegetation Dynamics in Sri Lankan Mangroves as Detected from Sequential Aerial Photography: A Case Study in Galle." *Bulletin of Marine Science* 672: 741–59.

Dahdouh-Guebas, F., T. Zetterström, P. Rönnback, M. Troell, A. Wickramasinghe, and N. Koedam. 2002. "Recent Changes in Land-Use in the Pambala-Chilaw Lagoon Complex Sri Lanka, Investigated Using Remote Sensing and GIS: Conservation of Mangroves vs. Development of Shrimp Farming." *Environment, Development and Sustainability* 42: 185–200.

De Boer, W. F. 2002. "The Rise and Fall of the Mangrove Forests in Maputo Bay, Mozambique." *Wetlands Ecology and Management* 10: 313–22.

Dittmar, T., N. Hertkorn, G. Kattner, and R. J. Lara. 2006. "Mangroves, a Major Source of Dissolved Organic Carbon to the Oceans." *Global Biogeochemical Cycles* 20: 1–7.

Donato, D. C., J. B. Kauffman, D. Murdiyarso, S. Kurnianto, M. Stidham, and M. Kanninen. 2011. "Mangroves among the Most Carbon-Rich Tropical Forests and Key in Land-Use Carbon Emissions." *Nature Geoscience* 4: 293–7.

FAO (Food and Agriculture Organization of the United Nations). 2007. *Mangroves of Africa 1980–2005: Country Reports.* Forest Resources Assessment Working Paper No. 135. Rome: FAO.

Farr, T. G., P. A. Rosen, E. Caro, R. T. Crippen, R. Duren, S. Hensley, M. Kobrick, M. Paller, E. Rodriguez, L. Roth, D. Seal, S. Shaffer, J. Shimada, J. Umland, M. Werner, M. Oskin, D. Burbank, and D. Alsdorf. 2007. "The Shuttle Radar Topography Mission." *Review of Geophysics* 45: 1–33.

Fatoyinbo, T. E., M. Simard, R. A. Washington-Allen, and H. H. Shugart. 2008. "Landscape-Scale Extent, Height, Biomass, and Carbon Estimation of Mozambique's Mangrove Forests with Landsat ETM+ and Shuttle Radar Topography Mission Elevation Data." *Journal of Geophysical Research* 113: 1–13.

Faunce, C. H., and J. E. Serafy. 2006. "Mangroves as Fish Habitat: 50 Years of Field Studies." *Marine Ecology Progress Series* 318: 1–18.

Gesche, K., B. Michael, W. Stefan, and B. Gerald. 2004. "Mapping Land Cover and Mangrove Structures with Remote Sensing Techniques: A Contribution to Asynoptic GIS in Support of Coastal Management in North Brazil." *Environmental Management* 34: 429–40.

Gillespie, T. W., B. R. Zutta, M. K. Early, and S. Saatchi. 2006. "Predicting and Quantifying the Structure of Tropical Dry Forests in South Florida and the Neotropics Using Spaceborne Imagery." *Global Ecology and Biogeography* 153: 225–36.

Giri, C., E. Ochieng, L. L. Tieszen, Z. Zhu, A. Singh, T. Loveland, J. Masek, and N. Duke. 2011. "Status and Distribution of Mangrove Forests of the World Using Earth Observation Satellite Data." *Global Ecology and Biogeography* 20: 154–9.

Green, E. P., C. D. Clark, P. J. Mumby, A. J. Edwards, and A. C. Ellis. 1998. "Remote Sensing Techniques for Mangrove Mapping." *International Journal of Remote Sensing* 19: 935–56.

Harding, D., and C. Carabajal. 2005. "ICESat Waveform Measurements of Within-Footprint Topographic Relief and Vegetation Vertical Structure." *Geophysical Research Letters* 32: 1–4.

Houghton, R. A., F. G. Hall, and S. J. Goetz. 2009. "Importance of Biomass in the Global Carbon Cycle." *Journal of Geophysical Research* 114: 1–13.

James, G. K., J. O. Adegoke, S. Ekechukwu, P. Nwilo, and J. Akinyede. 2007. "Satellite-Based Assessment of the Extent and Changes in the Mangrove Ecosystem of the Niger Delta." *Marine Geodesy* 30: 249–67.

Kellndorfer, J., W. Walker, L. Pierce, C. Dobson, J. A. Fites, C. Hunsaker, J. Vona, and M. Clutter. 2004. "Vegetation Height Estimation from Shuttle Radar Topography Mission and National Elevation Datasets." *Remote Sensing of Environment* 933: 339–58.

Kovacs, J. M., J. Wang, and M. Blanco-Correa. 2001. "Mapping Disturbances in a Mangrove Forest using Multi-date Landsat TM Imagery." *Environmental Management* 27, no. 5: 763–76.

Kruitwagen, G., H. Pratap, A. Covaci, and S. W. Bonga. 2008. "Status of Pollution in Mangrove Ecosystems along the Coast of Tanzania." *Marine Pollution Bulletin* 56: 1022–31.

Lefsky, M., D. Harding, M. Keller, W. Cohen, C. Carabajal, F. Del Bom Espirito-Santo, M. Hunter, R. De Oliveira Jr, and P. De Camargo. 2005. "Estimates of Forest Canopy Height and Aboveground Biomass Using ICESat." *Geophysical Research Letters* 32: 1–4.

Lefsky, M. A., M. Keller, Y. Pang, P. De Camargo, and M. O. Hunter. 2007. "Revised Method for Forest Canopy Height Estimation from the Geoscience Laser Altimeter System Waveforms." *Journal of Applied Remote Sensing* 1: 1–18.

Lucas, R. M., A. L. Mitchell, A. Rosenqvist, C. Proisy, A. Melius, and C. Ticehurst. 2007. "The Potential of L-Band SAR for Quantifying Mangrove Characteristics and Change: Case

Studies from the Tropics." *Aquatic Conservation: Marine and Freshwater Ecosystems* 173: 245–64.

North, P. R. J., J. A. B. Rosette, J. C. Suárez, and S. O. Los. 2010. "A Monte Carlo Radiative Transfer Model of Satellite Waveform LiDAR." *International Journal of Remote Sensing* 31: 1343–58.

Rodriguez, E., E. Morris, and J. E. Belz. 2006. "A Global Assessment of the SRTM Performance." *Photogrammetric Engineering & Remote Sensing* 723: 249–60.

Rosette, J. A. B., P. R. J. North, J. C. Suarez, and S. O. Los. 2010. "Uncertainty within Satellite LiDAR Estimations of Vegetation and Topography." *International Journal of Remote Sensing* 31: 1325–42.

Saenger, P., and M. F. Bellan. 1995. *The Mangrove Vegetation of the Atlantic Coast of Africa*. Toulouse: Université de Toulouse Press.

Saenger, P., and S. C. Snedaker. 1993. "Pantropical Trends in Mangrove Above-Ground Biomass and Annual Litterfall." *Oecologia* 96: 293–9.

Satyanarayana, B., B. Thierry, Lo D. Seen, A. V. Raman, and G. Muthusankar. 2001. "Remote Sensing in Mangrove Research-Relationship between Vegetation Indices and Dendrometric Parameters: A Case for Coringa, East Coast of India." In *Proceedings from the 22nd Asian Conference on Remote Sensing*, November 5–9, 2001. Singapore: Centre for Remote Imaging, Sensing and Processing.

Schutz, B. E., H. J. Zwally, C. A. Shuman, D. Hancock, and J. P. Dimarzio. 2005. "Overview of the ICESat Mission." *Geophysical Research Letters* 32: L21S01.

Simard, M., V. H. Rivera-Monroy, J. E. Mancera-Pineda, E. Castaneda-Moya, and R. R. Twilley. 2008. "A Systematic Method for 3D Mapping of Mangrove Forests Based on Shuttle Radar Topography Mission Elevation Data, ICESat/GLAS Waveforms and Field Data: Application to Cienaga Grande De Santa Marta, Colombia." *Remote Sensing of the Environment* 112: 2131–44.

Simard, M., K. Q. Zhang, V. H. Rivera-Monroy, M. S. Ross, P. L. Ruiz, E. Castaneda-Moya, R. R. Twilley, and E. Rodriguez. 2006. "Mapping Height and Biomass of Mangrove Forests in Everglades National Park with SRTM Elevation Data." *Photogrammetric Engineering & Remote Sensing* 723: 299–311.

Smith, G. M., T. Spencer, A. L. Murray, and J. R. French. 1998. "Assessing Seasonal Vegetation Change in Coastal Wetlands with Airborne Remote Sensing: An Outline Methodology." *Mangroves and Salt Marshes* 2: 15–28.

Spalding, M. D., F. Blasco, and C. D. Field, eds. 1997. *World Mangrove Atlas*. Okinawa: The International Society for Mangrove Ecosystems.

Sulong, I., H. Mohd-Lokman, K. Mohd-Tarmizi, and A. Ismail. 2002. "Mangrove Mapping Using Landsat Imagery and Aerial Photographs: Kema-man District, Terengganu, Malaysia." *Environment, Development and Sustainability* 4, no. 2: 135–52.

Tomlinson, P. B. 1994. *The Botany of Mangroves*. Cambridge: Cambridge University Press.

Traynor, C. H., and T. Hill. 2008. "Mangrove Utilisation and Implications for Participatory Forest Management, South Africa." *Conservation and Society* 62: 109–16.

Tucker, C. J., D. M. Grant, and J. D. Dykstra. 2004. "NASA's Global Orthorectified Landsat Data Set." *Photogrammetric Engineering & Remote Sensing* 703: 313–22.

Ukpong, I. E. 1995. "An Ordination Study of and Leaf Size Differences in Two Red Mangrove Swamp Communities in West Africa." *Vegetatio* 116: 147–59.

Wang, Y., B. Gregory, N. Jarunee, T. Michael, N. Amani, T. James, H. Lynne, B. Robert, and M. Vedast. 2003. "Remote Sensing of Mangrove Change along the Tanzania Coast." *Marine Geodesy* 26: 35–48.

Zwally, H. J., R. Schutz, C. Bentley, J. Bufton, T. Herring, J. Minster, J. Spinhirne, and R. Thomas. 2003. *GLAS/ICESat L2 Global Land Surface Altimetry Data V018*, October 15 to November 18, 2003. Boulder, CO: National Snow and Ice Data Center. Digital media.